Published in final edited form as:
J Neurosci Res. 2007 June ; 85(8): 1618–1627.

Expression of Insulin-Like Growth Factor System Genes During the Early Postnatal Neurogenesis in the Mouse Hippocampus

Jihui Zhang, **Billie M. Moats-Staats**, **Ping Ye**, and **A. Joseph D'Ercole***
Department of Pediatrics, University of North Carolina at Chapel Hill, Chapel Hill, North Carolina

Abstract

Insulin-like growth factor-1 (IGF-1) is essential to hippocampal neurogenesis and the neuronal response to hypoxia/ischemia injury. IGF (IGF-1 and -2) signaling is mediated primarily by the type 1 IGF receptor (IGF-1R) and modulated by six high-affinity binding proteins (IGFBP) and the type 2 IGF receptor (IGF-2R), collectively termed IGF system proteins. Defining the precise cells that express each is essential to understanding their roles. With the exception of IGFBP-1, we found that mouse hippocampus expresses mRNA for each of these proteins during the first 2 weeks of postnatal life. Compared to postnatal day 14 (P14), mRNA abundance at P5 was higher for IGF-1, IGFBP-2, -3, and -5 (by 71%, 108%, 100%, and 98%, respectively), lower for IGF-2, IGF-2R, and IGFBP-6 (by 65%, 78%, and 44%, respectively), and unchanged for IGF-1R and IGFBP-4. Using laser capture microdissection (LCM), we found that granule neurons and pyramidal neurons exhibited identical patterns of expression of IGF-1, IGF-1R, IGF-2R, IGFBP-2, and -4, but did not express other IGF system genes. We then compared IGF system expression in mature granule neurons and their progenitors. Progenitors exhibited higher mRNA levels of IGF-1 and IGF-1R (by 130% and 86%, respectively), lower levels of IGF-2R (by 72%), and similar levels of IGFBP-4. Our data support a role for IGF in hippocampal neurogenesis and provide evidence that IGF actions are regulated within a defined in vivo milieu.

Keywords

insulin-like growth factor (IGF); hippocampus; dentate gyrus; laser capture microdissection (LCM)

Insulin-like growth factor (IGF)-1 and -2 are highly homologous polypeptides that have major roles in the regulation of somatic growth (Baker et al., 1993; Efstratiadis, 1998; Lupu et al., 2001). Multiple lines of evidence indicate that IGF-1 is essential to normal brain growth and development (D'Ercole et al., 1996, 2002; Russo et al., 2005). IGF growth promoting effects are believed to be mediated primarily by the type 1 IGF receptor (IGF-1R), a membrane-spanning heterotetramer with intrinsic tyrosine kinase domains (Cohick and Clemmons, 1993; Dupont and LeRoith, 2001). The type 2 IGF receptor (IGF-2R), identical to the cation-independent mannose-6-phosphate receptor, is a transmembrane monomeric glycoprotein involved in endocytosis-mediated degradation of IGF-2 and intracellular trafficking of lysosomal enzymes (MacDonald et al., 1988). There is, however, a paucity of evidence indicating that the IGF-2R directly mediates IGF signaling. IGF actions also are modulated by six high-affinity IGF binding proteins (IGFBP-1 to -6), extracellular proteins that regulate the distribution and bioavailability of IGF (Clemmons, 1998; Baxter, 2000). Collectively, these 10 proteins often are termed the IGF system.

* Correspondence to: A. Joseph D'Ercole, Department of Pediatrics, CB 7039, University of North Carolina at Chapel Hill, Chapel Hill, NC 27599-7039. E-mail: ajd@med.unc.edu.

The hippocampal formation is a bilateral cortical structure associated with learning and memory, as well as with emotional and behavioral functions. It is comprised of the dentate gyrus, the hippocampus proper (Ammon's horn), and the subiculum. Contrasted with the six-layered architecture of neocortex, the phylogenetically old hippocampus is three-layered and contains two principal types of neurons: glutamatergic pyramidal neurons of the hippocampus proper and granule neurons of the dentate gyrus. The development of the dentate gyrus and hippocampus proper is a multistep process under the guidance of a complex genetic program (Forster et al., 2006). In rats, neurogenesis in the dentate gyrus begins with the formation of the dentate primordium at embryonic day 15 (E15). During the first several weeks of postnatal life granule neuronogenesis is active and most granule neurons form at this time, however, the generation of granule neurons in the dentate gyrus subgranular layer continues throughout adult life (Stanfield and Cowan, 1979; Altman and Bayer, 1990; Reznikov, 1991). In this study we focused on the first 2 postnatal weeks, a period of very active dentate neurogenesis that approximately corresponds to the mid-second through the mid-third trimester of human gestation (Humphrey, 1967). This is a time when premature infants are at risk of suffering hypoxia/ischemia injury, and the hippocampus is especially vulnerable to hypoxic/ischemic injury (Cervos-Navarro and Diemer, 1991). Understanding the molecular mechanisms involved in hippocampal neurogenesis and identifying potential neuroprotective and growth promoting factors are critical to the repair of neuronal damage and the restoration of function after hypoxia/ischemia injury.

There is increasing evidence that IGF-1 exerts a wide variety of effects on neural cells both in vivo and in vitro (D'Ercole et al., 1996; Russo et al., 2005). In the postnatal dentate gyrus, IGF-1 promotes neurogenesis and synaptogenesis by increasing the total number of neurons and synapses (O'Kusky et al., 2000). IGF-1-stimulated neuronal progenitor proliferation is achieved by an acceleration of the cell cycle, characterized by a decrease in the length of the G1 phase and increased cell cycle reentry (Hodge et al., 2004). Furthermore, animal studies have shown that increased IGF-1 expression is part of the physiologic response to brain hypoxia/ischemia injury and that administration of IGF-1 ameliorates such injuries (Gluckman et al., 1998; Guan et al., 2003).

Using a variety of techniques including in situ hybridization and ligand binding autoradiography, multiple laboratories have reported the localization of some components of IGF system in the hippocampus (Araujo et al., 1989; Werther et al., 1990; Yamaguchi et al., 1990; Bartlett et al., 1991; Aguado et al., 1993). These reports, however, are somewhat conflicting due to inherent limitations of these techniques. A complete delineation of the molecular mechanisms underlying IGF actions during hippocampal neurogenesis and development requires an understanding of the precise sites of IGF system gene expression. In this study we used laser capture microdissection (LCM) followed by reverse transcription-polymerase chain reaction (RT-PCR) to examine the expression of IGF system genes in hippocampal neurons.

MATERIALS AND METHODS

Animals and Reagents

Wild-type C57BL/6J mice used in this study were fed ad lib and maintained in the animal care facility of the University of North Carolina at Chapel Hill. Protocols involving these animals were approved by the Institutional Animal Care and Use Committee. A rabbit anti-mouse Ki67 monoclonal antibody and a biotinylated goat anti-rabbit IgG secondary antibody were both purchased from Vector Laboratories (Burlingame, CA). Qdot 565-streptavidin conjugates, Platinum Taq DNA polymerases, and a SuperScript III first-strand cDNA synthesis kit were obtained from Invitrogen (Carlsbad, CA). LCM caps were obtained from Arcturus (Mountain View, CA).

Immunofluorescence Staining

After sacrifice, brain tissues were removed quickly and dissected along the mid sagittal plane. Frozen sagittal sections were cut at 8-μm thickness and stored at −80°C, if not used immediately for immunostaining. Sections were fixed in cold acetone for 2 min, then rinsed twice in PBS containing 0.1% Triton X-100 (PBST). Ki67 primary antibodies diluted at 1:200 in PBS containing 2% BSA were applied for 30 min at room temperature. Slides were washed once in PBST and once in PBS for 5 min each. Biotinylated secondary antibodies diluted at 1:1,000 in PBS-2% BSA were applied for 15 min and followed by two separate washes in PBST and PBS. Sections were incubated with Qdot 565-streptavidin diluted at 1:100 in PBS-2% BSA for 30 min, washed twice in PBS for 5 min each, mounted with 90% glycerol, and observed under an Olympus BX60 fluorescence microscope.

Laser Capture Microdissection

For isolation of hippocampal pyramidal neurons and dentate gyrus granule neurons, we carried out laser capture microdissection (LCM) on frozen brain sections from P14 wild-type mice using a PixCell II system (Arcturus, Molecular Devices, Sunnyvale, CA). Sections were stained with a Histo-Gene LCM Frozen Section Staining Kit from Arcturus. Mature granule neurons were dissected along the center of the granular layer to avoid contamination of immature neurons residing in the subgranular layer. Pyramidal neurons were dissected along the pyramidal cell layer of hippocampus proper.

Granule neurons that were either Ki67-positive or negative also were procured by LCM on 8-μm frozen brain sections from P12 wild-type mice after immunostaining with anti-Ki67 antibodies. To preserve the integrity of RNAs on these sections, buffers used for immunostaining were prepared with nuclease-free water and the staining process was carried out at 4°C in a bench-top cooler. We also used a protocol requiring <15 min. This was accomplished by conducting antibody incubations no longer than needed for achieving specific staining. We were able to reduce the Ki67 primary antibody incubation to 3 min at 1:50 dilutions, the secondary antibody incubation to 2 min at 1:200 dilutions, and the Qdot 565-streptavidin incubation to 3 min at 1:75 dilutions. Washes in PBST or PBS between these incubations were replaced with quick rinses. Sections were dehydrated through a series of graded alcohol and xylene. Ki67-positive granule cells along the subgranular layer of dentate gyrus were dissected and pooled from several sections. Mature granule cells (i.e., Ki67-negative) were dissected from the granular layer, but away from the subgranular layer to avoid Ki67-positive cell contamination. We routinely obtained 50–100 microdissected cells for both Ki67-positive and negative granule cells in one LCM session. After LCM, these cells were subjected immediately to RNA isolation.

RNA Isolation From Whole Hippocampus and LCM Procured Cells

Mouse brains were removed quickly after sacrifice, hippocampal tissues were then dissected. They were flash-frozen in liquid nitrogen and stored subsequently at −80°C. Total RNA was isolated using an RNeasy Mini kit (Qiagen) with the protocol recommended by the manufacturer. RNA samples were dissolved in nuclease-free water and the concentrations were measured by UV spectrometry. For LCM samples, total RNA was isolated with a PicoPure RNA kit (Arcturus). Procedures outlined by the manufacturer were closely followed, including an optional step of in-column DNase digestion to remove genomic DNA.

Reverse Transcription and Polymerase Chain Reaction (RT-PCR)

One microgram of hippocampal RNA from each sample was subjected to reverse transcription using a SuperScript III first-strand cDNA synthesis kit. Both oligo$(dT)_{20}$ and random hexamers were used to prime the reverse transcription catalyzed by SuperScript III in the presence of

RNaseOUT. Reactions (20 μl/each) were incubated at 25°C for 10 min followed by 50 min of incubation at 50°C, then terminated at 85°C for 5 min. The resulting cDNA was diluted by 1:5, and 1 μl each was subjected to PCR. For LCM RNA samples (elution volume of 12 μl), 4 μl each were used for reverse transcription in 20 μl reactions as described above. Because the concentration of RNA in these samples was too low for quantification, the cDNA input for PCR was normalized to internal controls, GAPDH and β-actin.

PCR primers for IGF system genes and controls were designed according to published sequences in GenBank and are listed in Table I. Each pair of primers spans at least one intron in the corresponding gene. This enabled differentiation of cDNA amplicons from genomic DNA amplicons by size, if the latter were detected. For PCR with hippocampal cDNA as templates, each reaction contained 1 μl cDNA, amplification buffer containing 2.0 mM $MgCl_2$, 0.2 mM dNTPs, 0.5 μM sense and antisense primers, and 1 U Platinum Taq DNA polymerase. Annealing temperature was 57°C for IGFBP-5 and Ki67, 60°C for the other genes.

To ensure detection of rare mRNA, we first ran 40 PCR cycles for all genes on an Eppendorf MasterCycler and the products were visualized on agarose gels to show the amplification of each at its expected size. A series of PCR were then carried out to determine the number of cycles needed to reach the plateau phase for each gene. Semi-quantitative PCR were carried out with the same amount of cDNA input and with cycling terminated before the plateau phase was reached. Digital images of ethidium bromide stained gels were captured, and PCR products for each gene were quantified by optical densitometry using the Image-Pro Plus software (Media Cybernetics, Silver Spring, MD).

As the input of RNA from LCM samples in the reverse transcription reaction was not quantifiable, we calculated the cDNA amount for each sample based on their abundance of GAPDH and β-actin by PCR. Equivalent amount of cDNA was then used in PCR for each target gene as described above.

Data Analysis

The abundance of specific PCR products on gel images was measured in arbitrary optical density units. Data were analyzed after normalization to house-keeping genes by independent Student's *t*-test, and reported as a mean ± SEM. $P < 0.05$ was considered as demonstrating statistically significant difference.

RESULTS

Expression of IGF System Genes in the Postnatal Hippocampus

The first 2 weeks after birth comprise a period of significant hippocampal development in rodents, characterized by the growth and development of the dentate gyrus, including the birth of most granule neurons (Altman and Das, 1965; Stanfield and Cowan, 1979; Reznikov, 1991). Using a specific antibody against Ki67, a cell proliferation marker, we carried out immunostaining on sagittal brain sections from P5 and P14 mice. We observed widespread and intense staining in the dentate gyrus region at P5 (Fig. 1A). By the end of the second postnatal week, Ki67 immunostaining was greatly reduced and restricted to the subgranular layer (Fig. 1B), a location where progenitor proliferation continues at low levels throughout life (Kempermann et al., 2004; Forster et al., 2006). These changes in Ki67 expression was confirmed by RT-PCR (Fig. 1D).

Because P5 represents a period of rapid neurogenesis in the dentate gyrus whereas P14 is a time approaching adult steady state progenitor proliferation, we first surveyed the expression of IGF system genes in whole hippocampus by RT-PCR at these times. With the exception of IGFBP-1, PCR products of the expected size (Table I) were observed for all IGF system genes

(Fig. 1C,D), and sequence analyses confirmed the identity of each PCR amplicon. For IGFBP-1, however, RT-PCR showed a smaller product rather than the expected 354 bp amplicon. Sequence data showed a nucleotide sequence of 242 bp distinct from that of IGFBP-1 and thus ruled out the possibility of an alternatively spliced IGFBP-1 product. A BLAST search showed DNA sequences on mouse chromosome 13 that are nearly identical to the 242 bp amplicon, and homologous mRNA sequences also were reported in the EST database (data not shown). Our amplification of the 242 bp product is explained by the homology of our primers to sequences in this product despite 4 and 6 mismatches in the sense and the antisense primers, respectively, scattered at the 5′ ends of the primer sequences. To show that our IGFBP-1 primers can truly amplify specific IGFBP-1 sequences, we carried out RT-PCR with a RNA sample from the mouse liver, which is known to express IGFBP-1 (Ooi et al., 1990). Indeed, the expected 354 bp product was amplified, but not the nonspecific 242 bp product. In contrast, using hippocampus only the 242 bp product was amplified. When the annealing temperature was raised from 60°C to 65°C, amplification of the 242 bp product was reduced greatly, consistent with the mismatches in the primer region of the amplicon (Fig. 2A).

As IGF-1 gene contains an alternatively spliced exon 5 and when the reverse primer resides in this exon, the resulting PCR amplicon is 262 bp and represents the IGF-1B or -1C isoforms (Fig. 1), but not the more abundant IGF-1A isoform (Rotwein et al., 1986). To accurately measure total IGF-1 mRNA, therefore, we used primers that yield a 180 bp PCR product and amplify all IGF-1 mRNA isoforms. When duplex RT-PCR was carried out by combining the IGF-1 primers with the GAPDH primers in one reaction (using 60°C annealing temperature), both of the expected products were observed (Fig. 2B).

The expression of IGF-1 (the 180 bp product) and the other IGF system genes from P5 and P14 hippocampus were quantified densitometrically (Fig. 3). IGF-1, IGFBP-2, IGFBP-3, and IGFBP-5 were expressed at higher levels at P5 than at P14, whereas IGF-2, IGF-2R, and IGFBP-6 were expressed more highly at P14. No significant change in the expression of the IGF-1R or IGFBP-4 was observed. These data indicate that IGF system mRNA levels are highly variable and subjected to developmental regulation.

Expression of IGF System Genes in Granule Neurons and Pyramidal Neurons

When mature dentate gyrus granule neurons were isolated by LCM from the granular layer of P14 hippocampus sections, RT-PCR showed specific amplification for IGF-1, IGF-1R, IGF-2R, IGFBP-2, and IGFBP-4 (Fig. 4A–C). We failed, however, to detect IGF-2, IGFBP-3, -5, and -6. As expected, IGFBP-1 was not detected (not shown). Like in whole hippocampal tissue, IGFBP-4 was the most abundant IGFBP. Consistent with the literature (Kure and Brown, 1995), we found abundant expression of neurofilament light chain (NF-L) in these mature granule neurons. When RT-PCR were done with LCM-isolated pyramidal neurons, we found that the IGF system gene expression profile was identical to that of granule neurons (Fig. 4D–F), i.e., detection of IGF-1, IGF-1R, IGF-2R, IGFBP-2, and -4, but not IGFBP-1 (not shown), -3, -5, and -6. As expected, NF-L was also found to be expressed abundantly in these pyramidal neurons. To assess the degree of contamination by glial cells in these two groups of dissected neurons, we measured GFAP (an astrocyte marker) mRNA levels in these LCM samples and compared them with levels in LCM-dissected dentate gyrus. Although GFAP mRNA was highly abundant in the dentate gyrus, it was hardly detectable in granule neurons or pyramidal neurons (data not shown), indicating that glial cell contamination was minimal.

Expression of IGF System Genes in Mature and Immature Granule Neurons

Our next goal was to compare IGF system gene expression in immature and mature granule neurons, however, this goal posed significant problems. Because Ki67-positive cells are proliferating, they are by definition progenitors. In the postnatal dentate gyrus, Ki67-positive

cells are predominantly granule neuron progenitors, but precursors destined to a non-neuronal lineage may also be included in this population. Although Ki67-positive neurons are numerous in the dentate gyrus at P5, there is no clearly defined anatomic boundary between granular and subgranular layer that facilitates identification of relatively pure neuron and neuron progenitor populations (Fig. 1A). Furthermore, at P5 Ki67-negative cells are interspersed among Ki67-positive cells and this poses a different technical problem. Because Ki67 is a nuclear antigen, a Ki67-negative cell may in fact be positive if its nucleus is not (or partially) present on the 8-μm section. We elected, therefore, to study hippocampal sections at an older age when the dentate subgranular layer can be better recognized. We established criteria for identifying mature and immature granule neurons by combining Ki67 immunoreactivity and anatomic location, i.e., Ki67-positive cells in the subgranular layer as immature granule neurons and Ki67-negative cells deep in the granular layer as mature granule neurons. Given these considerations, we carried out our evaluation at P12, when Ki67-positive cells remain abundant (Fig. 5A) yet the granular and subgranular layers are well-defined.

Immature granule neurons along the subgranular layer were dissected (Fig. 5B,C) and pooled together from two or three sections. Mature granule neurons in the granular layer were then isolated from the same sections (Fig. 5D,E). Similar numbers of microdissected cells were collected for both immature and mature granule neurons, and successful RT-PCR amplifications were achieved with as few as 50 cells. We found that Ki67 mRNA expression was detected only in the immature granule neurons. As expected, the neuron progenitor marker double cortin also was only detected in immature granule neurons (Fig. 5F). For IGF system genes, we detected expression of IGF-1, IGF-1R, IGF-2R, and IGFBP-4 in both immature and mature granule neurons. We failed to amplify IGF-2, IGFBP-2, and -3 (Fig. 5, Panel G). Amplification also was not observed for IGFBP-1, -5, and -6 (not shown).

Because we observed IGFBP-2 expression in whole hippocampus at P5 and P14, and in P14 granule neurons, we questioned our failure to detect it in P12 granule neurons. When IGFBP-2 abundance was re-evaluated by RT-PCR using a greater number of P12 mature granule neuron, it was detected clearly (not shown). Unfortunately, due to their paucity, we were unable to obtain a similar number of Ki67-positive immature granule neurons at P12. We believe that IGFBP-2 is a low abundance mRNA in granule neuron and likely expressed in both immature and mature P12 granule neurons.

Compared to mature granule neurons, mRNA levels for IGF-1 and IGF-1R in immature granule neurons were higher by 130% (229.6 ± 36.8 vs. 100 ± 14.7, n = 4, $P < 0.01$) and 86% (185.9 ± 58.5 vs. 100 ± 36.4, n = 4, $P < 0.05$), respectively. IGF-2R mRNA level, however, was lower by 72% (27.9 ± 9.9 vs. 100 ± 17.8, n = 4, $P < 0.01$) in immature granule neurons. No significant change was observed for IGFBP-4 mRNA abundance (104 ± 9.7 vs. 100 ± 7.5, n = 4, $P = 0.46$).

DISCUSSION

We have examined the expression of IGF system genes in early postnatal mouse hippocampal formation with an emphasis on the dentate gyrus. Our studies were focused on the hippocampus at P5 and P14, two developmental ages that span a period critical to dentate gyrus development (Altman and Das, 1965; Stanfield and Cowan, 1979). We found that, with the exception of IGFBP-1, all other components of IGF system genes are expressed in the developing hippocampal formation. These mRNA levels are, however, highly variable and seem to be subjected to developmental regulation.

A complete understanding of IGF actions within a defined in vivo milieu, however, requires knowledge of the precise locations of IGF system gene expression. It is not surprising that considerable discrepancies exist regarding the localization of mRNAs of IGF system genes by

in situ hybridization (Araujo et al., 1989; Werther et al., 1990; Yamaguchi et al., 1990; Bartlett et al., 1991; Aguado et al., 1993), due to two major drawbacks of this technique: reliance on high abundance of mRNA (low sensitivity) and cross-hybridization of probes to non-specific transcripts (low specificity). LCM combined with RT-PCR offers precise isolation of cells of interest and high sensitivity and specificity. Using this technique, we were able to dissect mature granule neurons and mature pyramidal neurons from hippocampal sections. As most granule neurons are generated postnatally in mice, the period between P5–P14 provides a convenient span for isolation of mature granule neurons and their progenitors. Our RT-PCR data showed that these neurons also produce IGF-1, IGF-1R, and IGF-2R, and IGFBP-4 is the major binding protein produced by hippocampal neurons. Although higher levels of IGF-1 and IGF-1R were expressed in granule neuron progenitors, higher levels of IGF-2R were found in mature granule neurons.

In P5 hippocampal tissues, our study showed higher IGF-1 mRNA levels when compared to P14 hippocampal tissues. The expression of Ki67 greatly decreases by P14, consistent with a diminishing level of neurogenesis/cell proliferation in the hippocampus at this age. The expression pattern of IGF-1 correlates with the genesis of granule neurons in dentate gyrus, which peaks within the first postnatal week (P3–P5) and is decreased greatly at the end of second week, as shown by ^{3}H-thymidine labeling (Altman and Das, 1965; Stanfield and Cowan, 1979) and our Ki67 immunostaining. These findings suggest that IGF-1 produced locally plays an important role in hippocampal neurogenesis by paracrine and autocrine mechanisms. Although the IGF-1R expression in hippocampus was unchanged between P5 and P14, it likely remains sufficient to mediate IGF action.

In studies using in situ hybridization histochemistry, IGF-1 mRNA was detected in large polymorphic neurons, but not in CA pyramidal neurons of hippocampus proper. Similarly, in dentate gyrus IGF-1 mRNA was observed in polymorphic neurons of the hilus and neurons in the subgranular layer (Werther et al., 1990; Bartlett et al., 1991; Garcia-Segura et al., 1991). Using the LCM technique to precisely isolate dentate granule neurons and hippocampal pyramidal neurons followed by highly sensitive RT-PCR, we have shown that IGF-1 mRNA is expressed in both pyramidal and granule neurons, suggesting that the abundance of IGF-1 mRNA in these neurons is below the detection limit of in situ hybridization. In line with published data (using methods that detect either mRNA or protein) that IGF-1R is expressed in a variety of neuronal and glial cells (Araujo et al., 1989; Breese et al., 1991; Bondy et al., 1992; Aguado et al., 1993), our LCM data also show IGF-1R mRNA expression in both pyramidal and granule neurons. Compared to mature granule neurons, their immature progenitors expressed higher levels of both IGF-1 and the IGF-1R. We believe that neurons in the developing hippocampus not only respond to IGF-1, as evidenced by their expression of IGF-1R, they also produce IGF-1. This is supported by both in vitro and in vivo data indicating that IGF-1 effectively promotes hippocampal neuron progenitor proliferation and protects them from apoptosis (Cheng and Mattson, 1992; Aberg et al., 2000, 2003; O'Kusky et al., 2000; Cheng et al., 2001; Popken et al., 2004). The fact that primary cultured hippocampal neurons need exogenous IGF-1 to maintain their survival in vitro suggests that these neurons do not produce sufficient IGF-1 to protect them from apoptosis. Alternately, culture of these cells may diminish their capacity to express IGF-1, possibly because of the absence of regulatory signaling that occurs in vivo.

The expression of IGF-2 in the brain has been reported to be localized primarily to the choroid plexus (Hynes et al., 1988; Stylianopoulou et al., 1988; Sullivan and Feldman, 1994). Indeed, when the choroid plexus in the temporal horn of the lateral ventricle (adjacent to the hippocampus) was dissected by LCM, we found abundant IGF-2 mRNA expression (data not shown). We showed that the hippocampus expresses IGF-2 mRNA at both P5 and P14, with higher levels at P14. We failed, however, to detect IGF-2 mRNA in granule neurons or

pyramidal neurons by LCM, indicating other cells of synthesis. It seems possible that the increase of IGF-2 expression at P14 is associated with the development of hippocampal vasculature, because IGF-2 expression has been shown in both endothelial cells and vascular smooth muscle cells (Bar et al., 1988; Hagiwara et al., 1995; Bayes-Genis et al., 2000; Zaina et al., 2002; Ahmad et al., 2005).

Using a number of methods that detect either mRNA or protein, IGF-2R expression has been localized in the developing hippocampus (Smith et al., 1988; Breese et al., 1991; Couce et al., 1992; Kar et al., 1993; Hawkes and Kar, 2003). As with IGF-2, we found that IGF-2R mRNA abundance was higher in P14 hippocampus, compared to P5. We also found that the IGF-2R is expressed in pyramidal neurons and in both mature and progenitor granule neurons, with higher abundance in mature granule neurons than their progenitors. There is evidence that IGF-2R regulates cholinergic function in the hippocampus by activating G-protein sensitive protein kinase C (Hawkes et al., 2006), indicating a role in neuronal function other than internalization of IGF-2 or trafficking of lysosomal enzymes. Because IGF-2 is a secreted protein, it is possible, if not likely, that it is available to interact with the IGF-2R on hippocampal neurons.

Six high-affinity IGFBP play a significant role in controlling the bioavailability and the distribution of IGF, and thus in modulating their activity. Depending on the context of specific studies, these binding proteins may either inhibit or augment IGF actions (Clemmons, 1998; Baxter, 2000). IGFBP are secreted proteins, many of which are abundant in the circulation, and thus, can be immunochemically detected in multiple tissues regardless of the cellular sites of synthesis. Our finding of an absence of IGFBP-1 mRNA expression in the hippocampus provides a good example. IGFBP-1 is abundant in the circulation, and several studies have immunochemically shown IGFBP-1 protein in the brain (Ocrant et al., 1990; Bunn et al., 2005), despite the absence of IGFBP-1 mRNA reported here and by others (Murphy et al., 1990; Chernausek et al., 1993; Lee et al., 2001). Defining the precise cellular sites of IGFBP expression is likely to provide insights into the local actions (autocrine/paracrine) of IGFBP, as opposed to those exerted by IGFBP in the circulation, i.e., endocrine actions.

Among the expressed IGFBP in the hippocampus IGFBP-4 mRNA abundance was unchanged between P5 and P14, and IGFBP-6 was shown to be higher at P14, whereas IGFBP-2, -3, and -5 were detected at higher abundance at P5. It is noteworthy that IGFBP-5, a binding protein known to be capable of augmenting IGF-1 actions (Clemmons, 1998; Baxter, 2000), is expressed at higher abundance at P5 when active neurogenesis occurs in dentate gyrus (Altman and Das, 1965; Stanfield and Cowan, 1979).

Our LCM data showed that mRNA levels for IGFBP-3, -5, and -6 were below the limits of detection in dissected granule and pyramidal neurons, though they were readily detectable in hippocampal tissues. This implies that their mRNA levels in two hippocampal principal neurons are extremely low, if expressed at all. The sources of their expression, thus, are other types of cells in the hippocampus, and likely to be either vascular cells or glial cells. The expression of IGFBP-3 and 5 in either glial cells or vascular cells have been documented in the literature (Schmid et al., 1993; Cheng and Feldman, 1997; Delafontaine et al., 2004). Our LCM data further indicate that IGFBP-4 is the principal binding protein produced by pyramidal neurons, and by both granule neurons and their precursors. Recently, IGFBP-4 mRNA expression has been associated with neuron differentiation (Yu et al., 2006). A study using microarrays showed a dramatic increase in IGFBP-4 expression when cultured neural stem cells derived from fetal brain ($CD133^+$ cells) were induced to differentiate into mature neurons. This observation, however, may not be applicable to neurogenesis in dentate gyrus, because these CD133 precursors have multi-lineage potential, whereas granule neuron progenitors are lineage-committed precursors. IGFBP-2 also is expressed by both mature granule and

pyramidal neurons at P14, but at much lower abundance. The low abundance of IGFBP-2 explains our initial failure to detect IGFBP-2 mRNA in P12 granule neurons. When mRNA representing a greater number of P12 mature granule neurons was used, IGFBP-2 expression was evident. We believe that our inability to obtain a similar number of P12 immature granule neurons explains our failure to document IGFBP-2 expression in these cells.

As evidenced from our experience with IGFBP-2 mRNA, RT-PCR with LCM-derived mRNA also has limitations. Although these methods have much greater sensitivity than other methods, a threshold for detection remains, in part because the number of target cells that can be procured is often limited. Immunostaining procedures necessary to identify these cells are likely another factor limiting detection of specific mRNAs. The conditions imposed by these methods are often harsh and have the potential to promote RNA degradation. Nonetheless, RT-PCR after LCM provides a valid and powerful approach to document the cell specific expression of a gene. Studies using LCM and RT-PCR, however, can not absolutely exclude the expression of a specific gene.

In summary, our findings provide further evidence that IGF actions in the developing hippocampus are complex and highly regulated. Principal hippocampal neurons express IGF-1, both types of IGF receptors, and IGFBP-4 as the predominant binding protein. It has been shown previously that IGF-1 exerts dramatic effects on the dentate gyrus in mice overexpressing IGF-1 (O'Kusky et al., 2000; D'Ercole et al., 2002; Popken et al., 2004) and in mutant mice with blunted IGF-1 action or expression (D'Ercole et al., 1994; Beck et al., 1995; Ni et al., 1997). These data indicate that IGF-1 signaling through IGF-1R plays a critical role in neurogenesis of dentate granule neurons in early postnatal mice.

Acknowledgements

We thank the Microscopy Service Laboratory at the University of North Carolina for technical support in laser capture microdissection.

Contract grant sponsor: NIH; Contract grant number: HD008299.

References

Aberg MA, Aberg ND, Hedbacker H, Oscarsson J, Eriksson PS. Peripheral infusion of IGF-I selectively induces neurogenesis in the adult rat hippocampus. J Neurosci 2000;20:2896–2903. [PubMed: 10751442]

Aberg MA, Aberg ND, Palmer TD, Alborn AM, Carlsson-Skwirut C, Bang P, Rosengren LE, Olsson T, Gage FH, Eriksson PS. IGF-I has a direct proliferative effect in adult hippocampal progenitor cells. Mol Cell Neurosci 2003;24:23–40. [PubMed: 14550766]

Aguado F, Rodrigo J, Cacicedo L, Mellstrom B. Distribution of insulin-like growth factor-I receptor mRNA in rat brain. Regulation in the hypothalamo-neurohypophysial system. J Mol Endocrinol 1993;11:231–239. [PubMed: 8297478]

Ahmad AM, Burns J, Gardner R, Graham C. Delayed and disturbed morphogenesis of the umbilical blood vessels in insulin-like growth factor-II deficient conceptuses (Igf2m+/p−). Dev Dyn 2005;233:88–94. [PubMed: 15765507]

Altman J, Das GD. Autoradiographic and histological evidence of postnatal hippocampal neurogenesis in rats. J Comp Neurol 1965;124:319–335. [PubMed: 5861717]

Altman J, Bayer SA. Migration and distribution of two populations of hippocampal granule cell precursors during the perinatal and post-natal periods. J Comp Neurol 1990;301:365–381. [PubMed: 2262596]

Araujo DM, Lapchak PA, Collier B, Chabot JG, Quirion R. Insulin-like growth factor-1 (somatomedin-C) receptors in the rat brain: Distribution and interaction with the hippocampal cholinergic system. Brain Res 1989;484:130–138. [PubMed: 2540883]

Baker J, Liu JP, Robertson EJ, Efstratiadis A. Role of insulin-like growth factors in embryonic and postnatal growth. Cell 1993;75:73–82. [PubMed: 8402902]

Bar RS, Boes M, Dake BL, Booth BA, Henley SA, Sandra A. Insulin, insulin-like growth factors, and vascular endothelium. Am J Med 1988;85:59–70. [PubMed: 2973748]

Bartlett WP, Li XS, Williams M, Benkovic S. Localization of insulin-like growth factor-1 mRNA in murine central nervous system during postnatal development. Dev Biol 1991;147:239–250. [PubMed: 1879610]

Baxter RC. Insulin-like growth factor (IGF)-binding proteins: Interactions with IGFs and intrinsic bioactivities. Am J Physiol Endocrinol Metab 2000;278:E967–76. [PubMed: 10826997]

Bayes-Genis A, Conover CA, Schwartz RS. The insulin-like growth factor axis: a review of atherosclerosis and restenosis. Circ Res 2000;86:125–130. [PubMed: 10666406]

Beck KD, Powell-Braxton L, Widmer HR, Valverde J, Hefti F. Igf1 gene disruption results in reduced brain size, CNS hypomyelination, and loss of hippocampal granule and striatal parvalbumin-containing neurons. Neuron 1995;14:717–730. [PubMed: 7718235]

Bondy C, Werner H, Roberts CT Jr, LeRoith D. Cellular pattern of type-I insulin-like growth factor receptor gene expression during maturation of the rat brain: Comparison with insulin-like growth factors I and II. Neuroscience 1992;46:909–923. [PubMed: 1311816]

Breese CR, D'Costa A, Booze RM, Sonntag WE. Distribution of insulin-like growth factor 1 (IGF-1) and 2 (IGF-2) receptors in the hippocampal formation of rats and mice. Adv Exp Med Biol 1991;293:449–458. [PubMed: 1662866]

Bunn RC, King WD, Winkler MK, Fowlkes JL. Early developmental changes in IGF-I, IGF-II, IGF binding protein-1, and IGF binding protein-3 concentration in the cerebrospinal fluid of children. Pediatr Res 2005;58:89–93. [PubMed: 15774848]

Cervos-Navarro J, Diemer NH. Selective vulnerability in brain hypoxia. Crit Rev Neurobiol 1991;6:149–182. [PubMed: 1773451]

Cheng B, Mattson MP. IGF-I and IGF-II protect cultured hippocampal and septal neurons against calcium-mediated hypoglycemic damage. J Neurosci 1992;12:1558–1566. [PubMed: 1313498]

Cheng CM, Cohen M, Tseng V, Bondy CA. Endogenous IGF1 enhances cell survival in the postnatal dentate gyrus. J Neurosci Res 2001;64:341–347. [PubMed: 11340640]

Cheng HL, Feldman EL. Insulin-like growth factor-I (IGF-I) and IGF binding protein-5 in Schwann cell differentiation. J Cell Physiol 1997;171:161–167. [PubMed: 9130463]

Chernausek SD, Murray MA, Cheung PT. Expression of insulin-like growth factor binding protein-4 (IGFBP-4) by rat neural cells-comparison to other IGFBPs. Regul Pept 1993;48:123–132. [PubMed: 7505459]

Clemmons DR. Role of insulin-like growth factor binding proteins in controlling IGF actions. Mol Cell Endocrinol 1998;140:19–24. [PubMed: 9722163]

Cohick WS, Clemmons DR. The insulin-like growth factors. Annu Rev Physiol 1993;55:131–153. [PubMed: 8466170]

Couce ME, Weatherington AJ, McGinty JF. Expression of insulin-like growth factor-II (IGF-II) and IGF-II/mannose-6-phosphate receptor in the rat hippocampus: An in situ hybridization and immunocyto-chemical study. Endocrinology 1992;131:1636–1642. [PubMed: 1396308]

Delafontaine P, Song YH, Li Y. Expression, regulation, and function of IGF-1, IGF-1R, and IGF-1 binding proteins in blood vessels. Arterioscler Thromb Vasc Biol 2004;24:435–244. [PubMed: 14604834]

D'Ercole AJ, Ye P, Calikoglu AS, Gutierrez-Ospina G. The role of the insulin-like growth factors in the central nervous system. Mol Neurobiol 1996;13:227–255. [PubMed: 8989772]

D'Ercole AJ, Ye P, O'Kusky JR. Mutant mouse models of insulin-like growth factor actions in the central nervous system. Neuropeptides 2002;36:209–220. [PubMed: 12359511]

D'Ercole AJ, Dai Z, Xing Y, Boney C, Wilkie MB, Lauder JM, Han VK, Clemmons DR. Brain growth retardation due to the expression of human insulin like growth factor binding protein-1 in transgenic mice: An in vivo model for the analysis of IGF function in the brain. Brain Res Dev Brain Res 1994;82:213–222.

Dupont J, LeRoith D. Insulin and insulin-like growth factor I receptors: Similarities and differences in signal transduction. Horm Res 2001;55(Suppl 2):22–26. [PubMed: 11684871]

Efstratiadis A. Genetics of mouse growth. Int J Dev Biol 1998;42:955–976. [PubMed: 9853827]

Forster E, Zhao S, Frotscher M. Laminating the hippocampus. Nat Rev Neurosci 2006;7:259–267. [PubMed: 16543914]

Garcia-Segura LM, Perez J, Pons S, Rejas MT, Torres-Aleman I. Localization of insulin-like growth factor I (IGF-I)-like immunoreactivity in the developing and adult rat brain. Brain Res 1991;560:167–174. [PubMed: 1722132]

Gluckman PD, Guan J, Williams C, Scheepens A, Zhang R, Bennet L, Gunn A. Asphyxial brain injury —the role of the IGF system. Mol Cell Endocrinol 1998;140:95–99. [PubMed: 9722175]

Guan J, Bennet L, Gluckman PD, Gunn AJ. Insulin-like growth factor-1 and post-ischemic brain injury. Prog Neurobiol 2003;70:443–462. [PubMed: 14568359]

Hagiwara K, Kobayashi T, Tobita M, Kikyo N, Yazaki Y, Okabe T. Isolation of a cDNA for a growth factor of vascular endothelial cells from human lung cancer cells: Its identity with insulin-like growth factor II. Jpn J Cancer Res 1995;86:202–207. [PubMed: 7730145]

Hawkes C, Kar S. Insulin-like growth factor-II/mannose-6-phosphate receptor: widespread distribution in neurons of the central nervous system including those expressing cholinergic phenotype. J Comp Neurol 2003;458:113–127. [PubMed: 12596253]

Hawkes C, Jhamandas JH, Harris KH, Fu W, MacDonald RG, Kar S. Single transmembrane domain insulin-like growth factor-II/mannose-6-phosphate receptor regulates central cholinergic function by activating a G-protein-sensitive, protein kinase C-dependent pathway. J Neurosci 2006;26:585–596. [PubMed: 16407557]

Hodge RD, D'Ercole AJ, O'Kusky JR. Insulin-like growth factorI accelerates the cell cycle by decreasing G1 phase length and increases cell cycle reentry in the embryonic cerebral cortex. J Neurosci 2004;24:10201–10210. [PubMed: 15537892]

Humphrey T. The development of the human hippocampal fissure. J Anat 1967;101:655–676. [PubMed: 6059818]

Hynes MA, Brooks PJ, Van Wyk JJ, Lund PK. Insulin-like growth factor II messenger ribonucleic acids are synthesized in the choroid plexus of the rat brain. Mol Endocrinol 1988;2:47–54. [PubMed: 3398842]

Kar S, Chabot JG, Quirion R. Quantitative autoradiographic localization of [125I]insulin-like growth factor I, [125I]insulin-like growth factor II, and [125I]insulin receptor binding sites in developing and adult rat brain. J Comp Neurol 1993;333:375–397. [PubMed: 8349849]

Kempermann G, Jessberger S, Steiner B, Kronenberg G. Milestones of neuronal development in the adult hippocampus. Trends Neurosci 2004;27:447–452. [PubMed: 15271491]

Kure R, Brown IR. Expression of low-molecular-weight neurofilament (NF-L) mRNA during postnatal development of the mouse brain. Neurochem Res 1995;20:833–846. [PubMed: 7477677]

Lee CI, Goldstein O, Han VK, Tarantal AF. IGF-II and IGF binding protein (IGFBP-1, IGFBP-3) gene expression in fetal rhesus monkey tissues during the second and third trimesters. Pediatr Res 2001;49:379–387. [PubMed: 11228264]

Lupu F, Terwilliger JD, Lee K, Segre GV, Efstratiadis A. Roles of growth hormone and insulin-like growth factor 1 in mouse postnatal growth. Dev Biol 2001;229:141–162. [PubMed: 11133160]

MacDonald RG, Pfeffer SR, Coussens L, Tepper MA, Brocklebank CM, Mole JE, Anderson JK, Chen E, Czech MP, Ullrich A. A single receptor binds both insulin-like growth factor II and mannose-6-phosphate. Science 1988;239:1134–1137. [PubMed: 2964083]

Murphy LJ, Seneviratne C, Ballejo G, Croze F, Kennedy TG. Identification and characterization of a rat decidual insulin-like growth factor-binding protein complementary DNA. Mol Endocrinol 1990;4:329–336. [PubMed: 1691820]

Ni W, Rajkumar K, Nagy JI, Murphy LJ. Impaired brain development and reduced astrocyte response to injury in transgenic mice expressing IGF binding protein-1. Brain Res 1997;769:97–107. [PubMed: 9374277]

Ocrant I, Fay CT, Parmelee JT. Characterization of insulin-like growth factor binding proteins produced in the rat central nervous system. Endocrinology 1990;127:1260–1267. [PubMed: 1696881]

O'Kusky JR, Ye P, D'Ercole AJ. Insulin-like growth factor-I promotes neurogenesis and synaptogenesis in the hippocampal dentate gyrus during postnatal development. J Neurosci 2000;20:8435–8442. [PubMed: 11069951]

Ooi GT, Orlowski CC, Brown AL, Becker RE, Unterman TG, Rechler MM. Different tissue distribution and hormonal regulation of messenger RNAs encoding rat insulin-like growth factor-binding proteins-1 and -2. Mol Endocrinol 1990;4:321–328. [PubMed: 1691819]

Popken GJ, Hodge RD, Ye P, Zhang J, Ng W, O'Kusky JR, D'Ercole AJ. In vivo effects of insulin-like growth factor-I (IGF-I) on prenatal and early postnatal development of the central nervous system. Eur J Neurosci 2004;19:2056–2068. [PubMed: 15090033]

Reznikov KY. Cell proliferation and cytogenesis in the mouse hippocampus. Adv Anat Embryol Cell Biol 1991;122:1–74. [PubMed: 1927657]

Rotwein P, Pollock KM, Didier DK, Krivi GG. Organization and sequence of the human insulin-like growth factor I gene. alternative RNA processing produces two insulin-like growth factor I precursor peptides. J Biol Chem 1986;261:4828–4832. [PubMed: 2937782]

Russo VC, Gluckman PD, Feldman EL, Werther GA. The insulin-like growth factor system and its pleiotropic functions in brain. Endocr Rev 2005;26:916–943. [PubMed: 16131630]

Schmid C, Schlapfer I, Waldvogel M, Peter M, Zapf J, Froesch ER. Production of IGFBP-3 by connective tissue and endothelial cells. Growth Regul 1993;3:65–67. [PubMed: 7683535]

Smith M, Clemens J, Kerchner GA, Mendelsohn LG. The insulin-like growth factor-II (IGF-II) receptor of rat brain: Regional distribution visualized by autoradiography. Brain Res 1988;445:241–246. [PubMed: 2967099]

Stanfield BB, Cowan WM. The development of the hippocampus and dentate gyrus in normal and reeler mice. J Comp Neurol 1979;185:423–459. [PubMed: 86549]

Stylianopoulou F, Herbert J, Soares MB, Efstratiadis A. Expression of the insulin-like growth factor II gene in the choroid plexus and the leptomeninges of the adult rat central nervous system. Proc Natl Acad Sci U S A 1988;85:141–145. [PubMed: 3422410]

Sullivan KA, Feldman EL. Immunohistochemical localization of insulin-like growth factor-II (IGF-II) and IGF-binding protein-2 during development in the rat brain. Endocrinology 1994;135:540–547. [PubMed: 7518384]

Werther GA, Abate M, Hogg A, Cheesman H, Oldfield B, Hards D, Hudson P, Power B, Freed K, Herington AC. Localization of insulin-like growth factor-I mRNA in rat brain by in situ hybridization-relationship to IGF-I receptors. Mol Endocrinol 1990;4:773–778. [PubMed: 2177145]

Yamaguchi F, Itano T, Mizobuchi M, Miyamoto O, Janjua NA, Matsui H, Tokuda M, Ohmoto T, Hosokawa K, Hatase O. Insulin-like growth factor I (IGF-I) distribution in the tissue and extracellular compartment in different regions of rat brain. Brain Res 1990;533:344–347. [PubMed: 2289149]

Yu S, Zhang JZ, Xu Q. Genes associated with neuronal differentiation of precursors from human brain. Neuroscience 2006;141:817–825. [PubMed: 16809006]

Zaina S, Pettersson L, Ahren B, Branen L, Hassan AB, Lindholm M, Mattsson R, Thyberg J, Nilsson J. Insulin-like growth factor II plays a central role in atherosclerosis in a mouse model. J Biol Chem 2002;277:4505–4511. [PubMed: 11726660]

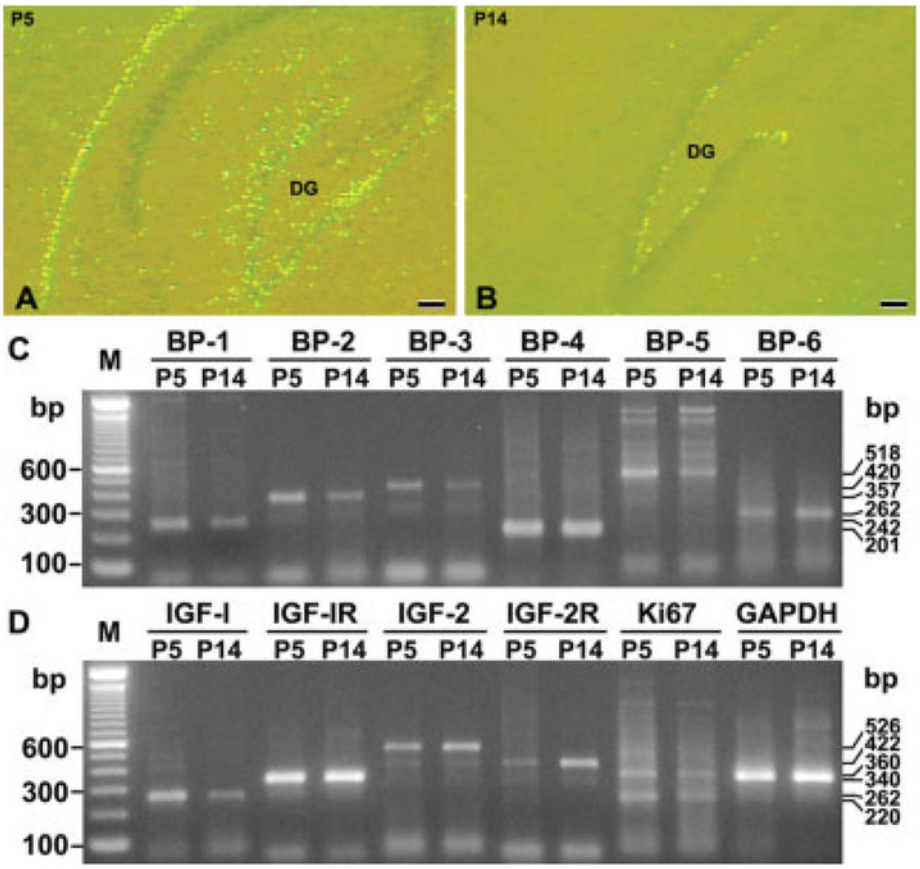

Fig. 1.

Ki67 immunostaining and RT-PCR amplification of IGF system genes in the developing hippocampal formation of early post-natal mice. Hippocampal Ki67-immunostaining was carried out on sagittal brain sections from either P5 (**A**) or P14 (**B**) WT mice. Ki67-positive cells shown in green fluorescence were wide spread in the dentate gyrus (DG) region at P5, but restricted into the subgranular layer at P14. Expression of IGF system genes in P5 and P14 hippocampus is represented in (**C**) and (**D**). RT-PCR for IGFBP-1 gave rise to a product of 242 bp, instead of the expected size of 354 bp. The rest of the IGF system genes were specifically amplified and of the predicted size: IGFBP-2, 357 bp; IGFBP-3, 420 bp; IGFBP-4, 201 bp; IGFBP-5, 518 bp; IGFBP-6 and IGF-1, 262 bp; IGF-2, 526 bp; IGF-1R, 340 bp; and IGF-2R, 422 bp. PCR products with expected size of 220 bp and 360 bp also were obtained for Ki67 and GAPDH, respectively. For IGFBP-5 and Ki67, non-specific amplification was detected in addition to the predicted bands, likely due to a relatively low annealing temperature used for these two pairs of primer, which failed to amplify their specific targets above 57°C. Consistent with the observation that there are significantly greater numbers of Ki67-positive cells at P5 than at P14, Ki67 mRNA levels were much higher at P5 when compared to that at P14. GAPDH, studied as an internal control for RT-PCR, did not exhibit significant changes between P5 and P14. Scale bar =100 μm. [Color figure can be viewed in the online issue, which is available at www.interscience.wiley.com.]

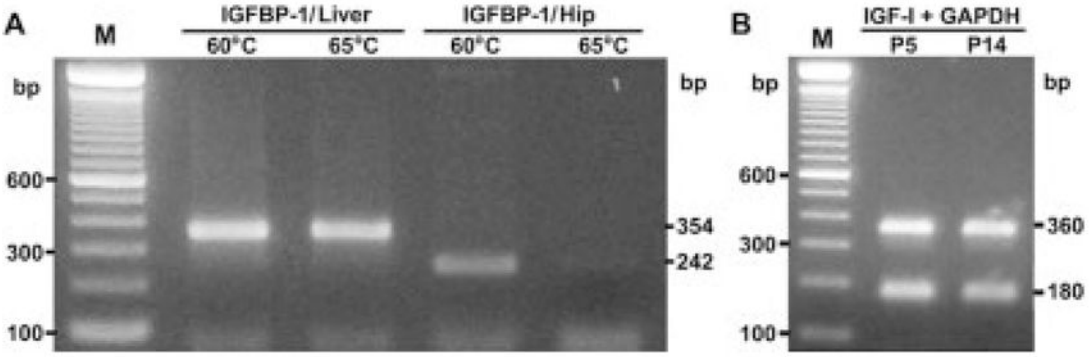

Fig. 2.

Amplification of IGFBP-1 and total IGF-1 by RT-PCR. RT-PCR for IGFBP-1 were carried out with RNA samples from both liver and hippocampus (**A**). As expected, the specific 354 bp IGFBP-1 product was detected from liver RNA. A smaller product of 242 bp was amplified from hippocampal RNA and the expected 354 bp product was not amplified. Sequencing of the 242 bp DNA showed that it resulted from non-specific amplification, and this confirms that we could not detect IGFBP-1 expression in the hippocampus. **B:** Duplex PCR of IGF-1 (180 bp) and GAPDH (360 bp) with RNA samples from P5 and P14 hippocampal tissues. This pair of IGF-1 primers detects all IGF-1 isoforms and reflects total IGF-1 mRNA levels, whereas the primers used in Figure 1 only detect IGF-1 mRNA isoforms that contain exon 5.

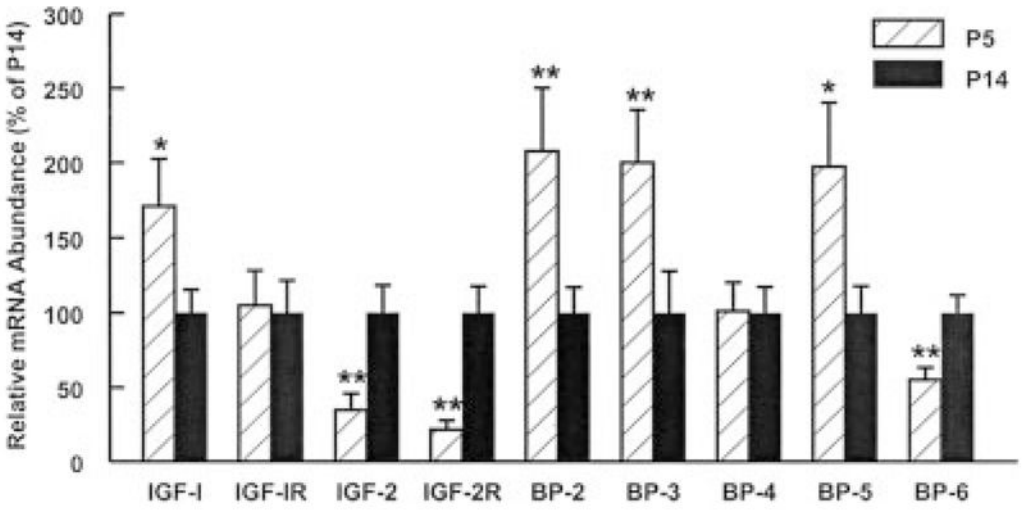

Fig. 3.

Relative quantification of mRNA levels for IGF system genes in P5 and P14 hippocampus. Levels of IGF system gene expression in P5 and P14 hippocampus were quantified by gel densitometry after RT-PCR. P5 hippocampal mRNA levels for IGF-1 (30 cycles), IGFBP-2 (33 cycles), -3 (33 cycles), and -5 (37 cycles) were higher by 71%, 108%, 100%, and 98%, respectively; whereas those for IGF-2 (30 cycles), IGF-2R (36 cycles), and IGFBP-6 (37 cycles) were lower by 65%, 78%, and 44%, respectively, when compared to their mRNA levels at P14. No significant changes were observed for IGF-1R (30 cycles) and IGFBP-4 (32 cycles). For IGF-1, the 180 bp PCR product represents all IGF-1 mRNA isoforms. Data are presented as mean ± SEM; n =4. $*P < 0.05$; $**P < 0.01$.

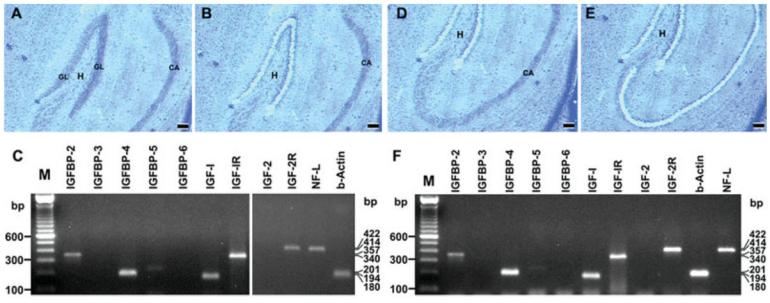

Fig. 4.

Profiling of mRNAs for IGF system genes in hippocampal pyramidal neurons and dentate gyrus granule neurons. Dentate granule neurons were isolated from 8 μm sagittal sections from a P14 mouse brain by LCM. Microdissections were carried out deep in the granular layer to avoid immature granule neurons in the subgranular layer (**A**,**B**; showing sections before and after microdissection, respectively). From the same sections, pyramidal neurons of hippocampus proper were then dissected (**D**,**E**; showing sections before and after microdissection, respectively). RT-PCR were carried out for IGF system genes with RNA samples from granule neurons (**C**) or pyramidal neurons (**F**). Identical patterns of IGF system gene expression were observed for both types of neurons, with detection of IGFBP-2 (357 bp), IGFBP-4 (201 bp), IGF-1 (180 bp), IGF-1R (340 bp), IGF-2R (422 bp); but not other components of IGF system. NF-L (414 bp) and β-actin (194 bp) were also detected in both types of neurons. Scale bar =100 μm. GL, granular layer; H, hilus; CA, Cornu Ammonis. [Color figure can be viewed in the online issue, which is available at www.interscience.wiley.com.]

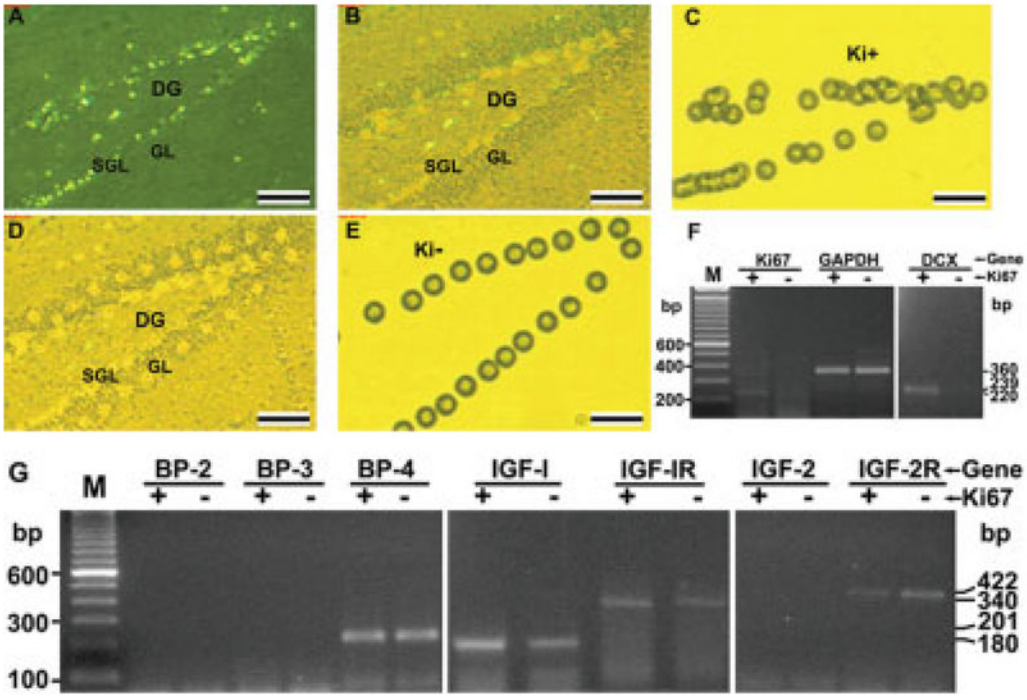

Fig. 5.

mRNA expression of IGF system genes in immature and mature granule neurons. Ki67 immunohistochemistry was carried out on 8-μm frozen sagittal sections from P12 mouse brains. Positive cells shown with green fluorescence were clustered along the subgranular layer of dentate gyrus (**A**), and were considered immature granule neurons. They were first dissected by LCM (**B** shows where microdissected cells were captured on the section; **C** shows the same cells that were captured for analysis). Next, Ki67-negative cells in the granular layer (i.e., mature granule neurons) were collected from the same sections (**D** shows where microdissected cells were captured on the section; **E** shows the same cells that were captured for analysis). RT-PCR showed detection of both Ki67 (220 bp) and double cortin (DCX, 239 bp) mRNAs exclusively in immature granule neurons (**F**). Expression of IGF system genes in mature and immature granule neurons were determined by RT-PCR and shown in gels at the bottom (**G**). Amplification of IGFBP-4 (201 bp), IGF-1 (180 bp), IGF-1R (340 bp), and IGF-2R (422 bp) was observed in both mature and immature granule neurons. Other IGF system genes were not detected. Scale bar = 100 μm. DG, dentate gyrus; SGL, subgranular layer; GL, granular layer; +, Ki67-positive; −, Ki67-negative. [Color figure can be viewed in the online issue, which is available at www.interscience.wiley.com.]

TABLE I

Primers for RT-PCR to Identify the Expression of IGF System Genes

Gene	GenBank Accession No.	Primers	Sizes of PCR amplicons	
			cDNA template	Genomic DNA template
IGF-I	NM_184052	5′-ACCGAGGGGCTTTTACTTCA-3′ (nt 1496 – nt 1515 in exon 3) 5′-TGGCTCACCTTTCCTTCTCC-3′ (nt 1757 – nt 1738 in exon 5)	262 bp	>50 kb
		5′-CTGGTGGATGCTCTTCAGTTCG-3′ (nt 1467 – nt 1488 in exon 3) 5′-TGCTTTTGTAGGCTTCAGTGGG-3′ (nt 1646 – nt 1625 in exon 4)	180 bp	>48 kb
IGF-IR	NM_010513	5′-GGAGAAGCCCATGTGTGAG-3′ (nt 561 – nt 579 in exon 2) 5′-GTCGTGGATAACGAAGCCATC-3′ (nt 900 – nt 880 in exon 3)	340 bp	>161 kb
IGF-II	NM_010514	5′-GATCCCAGTGGGGAAGTCG-3′ (nt 1131 – nt 1149 in exon 2) 5′-GCTGGACATCTCCGAAGAGGCTC-3′ (nt 1656 – nt 1634 in exon 4)	526 bp	1,978 bp
IGF-2R	NM_010515	5′-CCAACAGCTACCGGATGTCTG-3′ (nt 5942 – nt 5962 in exon 40) 5′-ATTCCCACCACAAGGATAGC-3′ (nt 6363 – nt 6344 in exon 42)	422 bp	1,921 bp
IGFBP-1	NM_008341	5′-CGAGATTTCTCGGCCTGCAG-3′ (nt 356 – nt 375 in exon 1) 5′-CTGATGGCGTTCCACAGGAT-3′ (nt 709 – nt 690 in exon 2)	354 bp	1,756 bp
IGFBP-2	NM_008342	5′-CTGAAGGCGCTTGTCACAGG-3′ (nt 401 – nt 420 in exon 1) 5′-AAGGCGCATGGTGGAGATCC-3′ (nt 757 – nt 738 in exon 3)	357 bp	>24 kb
IGFBP-3	NM_008343	5′-CAGGCAGCCTAAGCACCTAC-3′ (nt 446 – nt 465 in exon 1) 5′-AGCTCTGCTTTCTGCCTTTG-3′ (nt 865 – nt 846 in exon 4)	420 bp	4,930 bp
IGFBP-4	NM_010517	5′-GAAGCCATCCAGGAAAGCCTG-3′ (nt 556 – nt 576 in exon 1) 5′-CTCGCTCTGGCAGGAACCCT-3′ (nt 756 – nt 737 in exon 3)	201 bp	7,303 bp
IGFBP-5	NM_010518	5′-GATCAGCGTGGTCCTCCTG-3′ (nt 732 – nt 750 in exon 1) 5′-TGGGGTGGGCAGTGTTCTCT-3′ (nt 1249 – nt 1230 in exon 2)	518 bp	>10 kb
IGFBP-6	NM_008344	5′-GGTCTACAGCCCTAAGTGCG-3′ (nt 411 – nt 430 in exon 1) 5′-GCAGGGGCCCATCTCACTAT-3′ (nt 672 – nt 653 in exon 2&3)	262 bp	N/A
Ki67	XM_133912	5′-TGCAGAGAATGTCGGGATAAAG-3′ (nt 9410 – nt 9431 in exon 13) 5′-AGGAGATGGAGAAGTGAAGAGG-3′ (nt 9629 – nt 9608 in exon 15)	220 bp	4,333 bp
DCX	AB011678	5′-TCCCCAACACCTCAAAAGAC-3′ (nt 1127 – nt 1146 in exon 5) 5′-ATGGAATCGCCAAGTGAATC-3′ (nt 1365 – nt 1346 in exon 7)	239 bp	>12 kb
NF-L	NM_010910	5′-CTTGGACATCGAGATTGCAG-3′ (nt 1225 – nt 1244 in exon 2) 5′-GTGTCTTCCTCCTCACCCTC-3′ (nt 1638 – nt 1619 in exon 4)	414 bp	1,304 bp
GAPDH	M32599	5′-GTGTTCCTACCCCCAATGTG-3′ (nt 741 – nt 760 in exon 5) 5′-ATAGGGCCTCTCTTGCTCAG-3′ (nt 1100 – nt 1081 in exon 7)	360 bp	548 bp
b-Actin	NM_007393	5′-TGACGTTGACATCCGTAAAG-3′ (nt 935 – nt 954 in exon 4) 5′-ACAGTGAGGCCAGGATGGAG-3′ (nt 1128 – nt 1109 in exon 5)	194 bp	319 bp